JACS
JOURNAL OF THE AMERICAN CHEMICAL SOCIETY

Communication

pubs.acs.org/JACS

Phenylalanine Oligomers and Fibrils: The Mechanism of Assembly and the Importance of Tetramers and Counterions

Thanh D. Do, William M. Kincannon,[†] and Michael T. Bowers*

Department of Chemistry and Biochemistry, University of California, Santa Barbara, California 93106-9510, United States

Supporting Information

ABSTRACT: Phenylalanine is the only amino acid known to self-assemble into toxic fibrillar aggregates. An elevated concentration of phenylalanine in the blood can result in Phenylketonuria, a progressive mental retardation. Ion-mobility mass spectrometry is employed to investigate the structure and distribution of phenylalanine oligomers formed in the early stage of the aggregation cascade. The experimental cross sections indicate that phenyl-alanine self-assembles at neutral pH into oligomers composed of multiple layers of four monomers. The monomers arrange themselves to create a hydrophilic core made of zwitterionic termini and expose hydrophobic aromatic side chains to the outside. At high pH, the interactions between the neutral amino and negatively charged carboxylate of phenylalanine allow a minor population of ladder-like oligomers to be formed and detected in ion-mobility experiments. However, counterions such as ammonium rearrange those structures into the same structures observed at neutral pH. The cytotoxicity of Phe oligomers and fibrils may be due to favorable interactions between the hydrophobic exterior and the cell membrane and strong interactions between the hydrophilic core of Phe oligomers and ions, resulting in ion leakage and cellular damage.

Phenylketonuria is a metabolic disorder disease caused by an elevated concentration of phenylalanine (Phe) in the blood, originating from mutations in the gene encoding phenylalanine hydroxylase (PAH) located on chromosome 12.[1,2] Phe is also the building block of several artificial sweeteners (e.g., aspartame), which have been shown to cause severe side effects including neurological disorders, memory loss, and heart palpitations to those who have PAH genetic disorder.[3,4] It has also been recently established that Phe is the only amino acid capable of forming fiber-like aggregates with amyloid morphology at pathological concentrations.[5,6] Phe oligomers share similar characteristics to amyloid oligomers in terms of the cytotoxicity and responses to antibodies specifically designed to target amyloid formation.[7] Interestingly, it has been suggested that Phe fibrils interact with cells and that the fibrils can be found within the cells after incubation.[7] Recent experimental efforts to characterize the self-assembly and fibril formation process of Phe have been focused on the kinetics of fibril formation and the morphologies of aggregates at the end of the aggregation cascade.[6−9] Computational modeling, however, has provided valuable insights into the early structures of oligomers with potential to nucleate assembly (see Figure 1 for some possible structures of Phe oligomers).[7,10] Unfortunately traditional experimental methods are unable to capture important aspects of the metastable oligomer structures and hence cannot evaluate mechanisms proposed by theoretical studies due to the structural diversity of oligomers and the fast exchange between them.

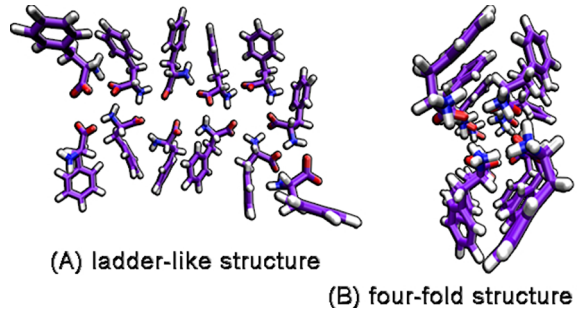

Figure 1. Proposed Phe oligomers obtained from MD simulations. (A) The ladder-like dodecamer extracted from the implicit solvent simulation of 27 NH_2−Phe−COO^- monomers by Caflisch and co-workers (ref 7); (B) the 4-fold dodecamer structure composed of three four-monomer layers obtained from the explicit solvent simulation by Hansmann and co-workers (ref 10).

In recent years, ion-mobility mass spectrometry (IM-MS) has evolved as a powerful analytical technique to study metastable and weakly bound complexes of biomolecules.[11−17] Under very soft electrospray ionization conditions in our instruments, solution-phase structures of peptide and protein oligomers can often be retained and characterized, as previously observed in a wide range of biological systems.[11,17−20] A combination of high level theoretical calculations and ion-mobility experiments makes it possible to obtain structural information on metastable oligomers at the molecular level.[21,22] In this Communication, IM-MS experiments are employed to characterize the self-assembly of Phe under a variety of experimental conditions. By characterizing a wide range of Phe oligomers (up to n = 60, where n is oligomer number), the mechanistic details of the assembly process can be unraveled, providing insights into the factors contributing to the stability and possibly to the cytotoxicity of the aggregates.

Figure 2 shows the ESI-quadrupole mass spectrum of 6 mM Phe in water (pH = 6.5). The mass spectrum shows the

Received: May 27, 2015
Published: August 5, 2015

DOI: 10.1021/jacs.5b05482
J. Am. Chem. Soc. 2015, 137, 10080−10083

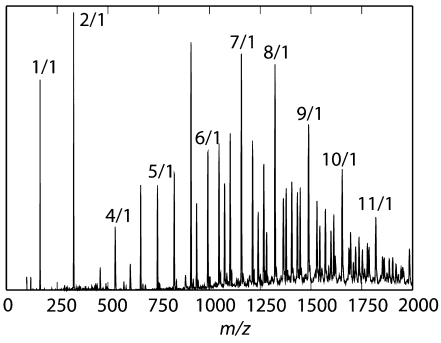

Figure 2. ESI-q mass spectrum of 6 mM Phe in water. The major mass spectral peaks are annotated with the smallest possible n/z, where n is the oligomer number and z is the charge. Each mass spectral peak may contain oligomers with different sizes (e.g., n/z = 4/1 contains both the singly charged tetramer n/z = 4/1 and the doubly charged octamer n/z = 8/2).

abundant formation of aggregates including singly and multiply charged oligomers (e.g., $[2(\text{Phe}) + \text{H}]^+$; n/z = 2/1 at 331 m/z, $[4(\text{Phe}) + \text{H}]^+$; n/z = 4/1 at 661 m/z, etc.). The earliest proposal for Phe self-assembly into fibril-like aggregates is from Caflisch and co-workers. Using molecular dynamics (MD) simulations they suggested that *neutral amino* Phe (NH_2−Phe-COO^-) at high pH can self-assemble into supramolecular fibrillar structures in which interactions between termini and counterions allow the formation of ladder-like Phe oligomers (see Figure 1A).[7] However, data presented elsewhere in the literature[6−9] are often of Phe in pure water (pH = 7) without counterions. Whether the formation of ladder-like oligomers provides a plausible pathway leading to aggregation at neutral pH remains in question. In order to address this concern, ion-mobility experiments were performed on mass-selected ions to measure their experimental collision cross sections. Representative arrival time distributions (ATDs) for $n \geq 4$ are shown in Figure 3.

The ATDs contain multiple features corresponding to oligomers at different sizes having the same m/z ratio. (Note: when oligomers populate the same m/z mass spectral peak, the largest oligomer arrives first, followed by the next largest, etc. in the order of its size to charge ratio.[23]) In all ATDs, the intensity of a higher-order oligomer is greater than that of the smallest oligomer. Together with the high intensities of the mass spectral peaks at high m/z (Figure 2), the data suggest that the formation of large-size oligomers is a very favorable process. The cross sections of metaclusters obtained from measuring ATDs of a mass spectral peak where the smallest oligomer is multiply charged (e.g., n/z = 13/2 at 1074 m/z, n/z = 15/2 at 1239 m/z, n/z = 17/2 at 1404 m/z, n/z = 19/3 at 1047 m/z, etc.) are consistent with the assignments for mass spectral peaks where the smallest oligomer can be singly charged (see Supporting Information Tables S1−2). Interestingly, the experimental cross sections appear to fit the growth trend predicted by the isotropic model[17] (see Figure 4) until n = 30 and show a positive deviation after that.

The experimental cross sections are significantly smaller than those of the ladder-like structures obtained from the simulation at high pH (see Figure 4A and Table S1), indicating ladder-like structures are not formed at neutral pH. The question thus remains as to the assembly mechanism at neutral pH that eventually leads to fibril formation.

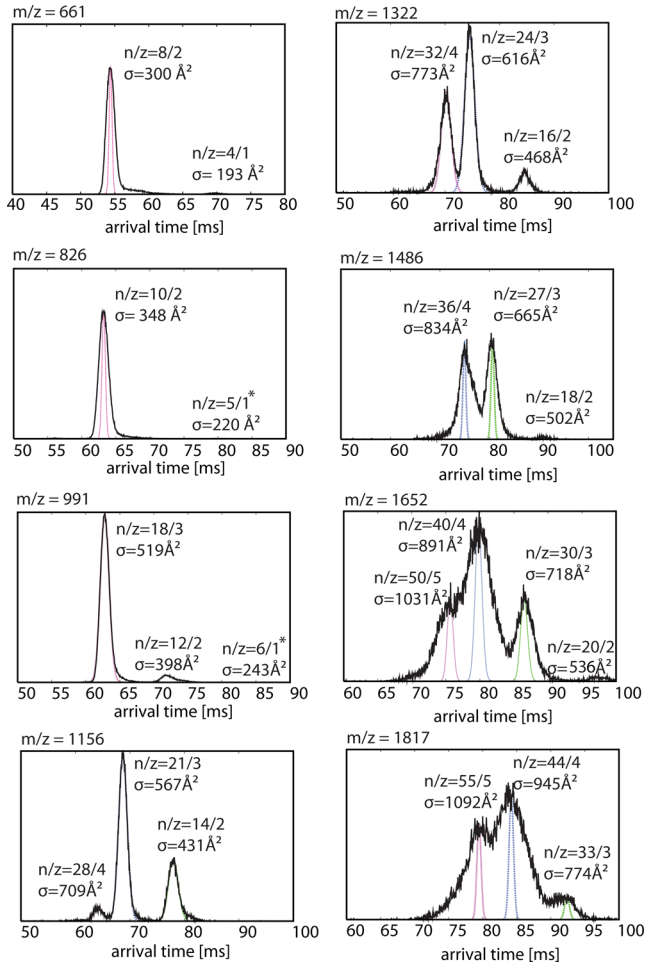

Figure 3. Representative ATDs of Phe mass spectral peaks starting from n/z = 4/1. Each ATD feature is annotated with n/z, where n is the oligomer number and z is the charge, and the experimental cross section. The feature corresponding to n = 5 and 6 (labeled with an asterisk) in the ATDs of the 826 m/z and 991 m/z mass spectral peak are visible but much less intense than the other features in the same ATDs. Underneath each experimental peak is a dotted line representing the peak shape for a single conformer at the indicated cross section.

A recent theoretical study by Hansmann and co-workers[10] suggests that zwitterionic Phe and diphenylalanine (FF) both self-assemble into amyloid-like aggregates through the formation of pore-like structures (i.e., nonladder-like structures; see Figure 1B) with 4-fold symmetry for Phe and 6-fold symmetry for FF oligomers. Since FF assembly into nanotubes involves the formation of hexagonal pores,[15,24,25] the possibility exists that Phe can self-assemble through the formation of multiple layers of four monomers (i.e., tetragonal pores, Figure 1B). To test this possibility we constructed the single-tube, double-tube, and tetra-tube pore-like models shown in Figure 4 based on the model of Hansmann.[10]

The experimental cross sections are compared to the growth trends predicted from the pore-like models (Figure 4C−E). The single-tube model shows good agreement to the experimental data up to n = 20, the double-tube model shows good agreement from n = 20 to 35, and the remaining data are well fit by the tetra-tube model. In the tetra-tube model, there are strong π-stacking interactions not only within each tube along the fibril axis (parallel π-stacking) but also

DOI: 10.1021/jacs.5b05482
J. Am. Chem. Soc. 2015, 137, 10080−10083

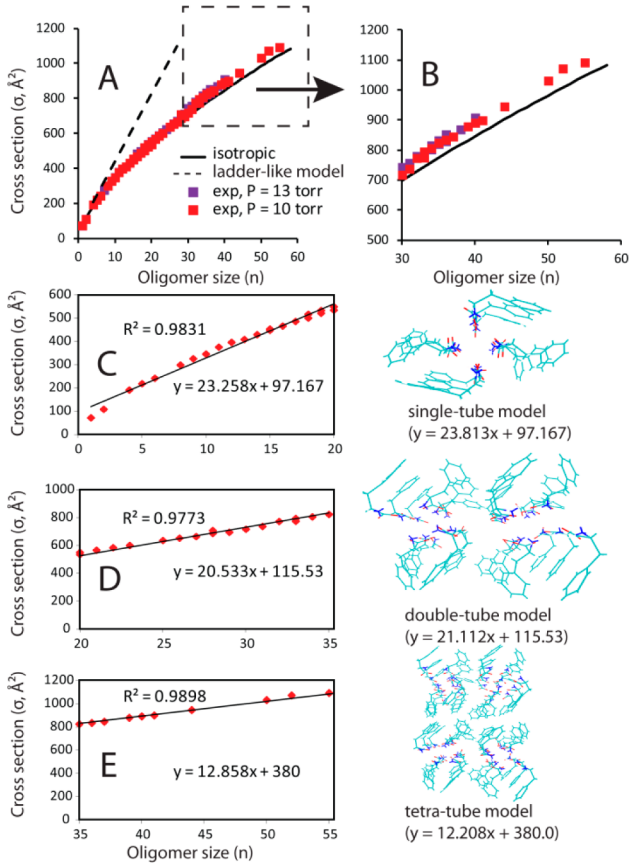

Figure 4. (A) Plot of oligomer number (n) versus experimental cross section (σ) for Phe metaclusters obtained from two independent experiments (P = 10 and 13 Torr). The experimental values are compared to predictions of the isotropic model $\sigma_n = \sigma_1 \times n^{2/3}$ (where σ_1 is the cross section of phenylalanine monomer, σ_1 = 73 Å^2), the ladder-like model, and the single/double-tube pore-like models. (B) A blow up of (A) showing the positive deviation from the isotropic model for n > 30. (C, D, E) Linear fit to determine the number of tubes concurrently growing and the representative structures of single-, double-, and tetra-tube models.

between the tubes in sideway directions (T-shaped π-stacking). This observation suggests that Phe fibrils prefer to grow and align themselves parallel to each other, consistent with previous microscopy imaging results.[6,7] Further, in this type of model the Phe oligomers would become more stable as size increases. This observation is consistent with the gradual increase in intensity of the ATD features as oligomers grow in size and the high intensities of mass spectral peaks at high m/z. The structures of large Phe oligomers (i.e., $n \geq 8$) resemble a steric zipper, a class of prefibrillar structures commonly found in amyloid peptides and proteins.[26] A major difference is the location of the dry (hydrophobic) and wet (hydrophilic) interfaces. In Phe oligomers, the hydrophilic region is buried inside while the outside is hydrophobic. In the amyloid steric zipper, the inside region is hydrophobic and the outside is hydrophilic. In addition, our data also suggest that Phe oligomers are formed by multiple layers of four monomers whereas steric zipper formation is often initiated by forming individual β-sheets.[17,27] These subtle differences could not have been understood without the ability to investigate the structures of *consecutive* oligomers as we have done above.

To investigate the self-assembly of Phe at high pH, we performed additional ion-mobility experiments in 20 mM ammonium acetate at both neutral and high pH. Ammonium acetate buffer is ESI friendly, and an ammonium cation NH_4^+ has the same charge as a Na^+. We show in Figure 5A–B the

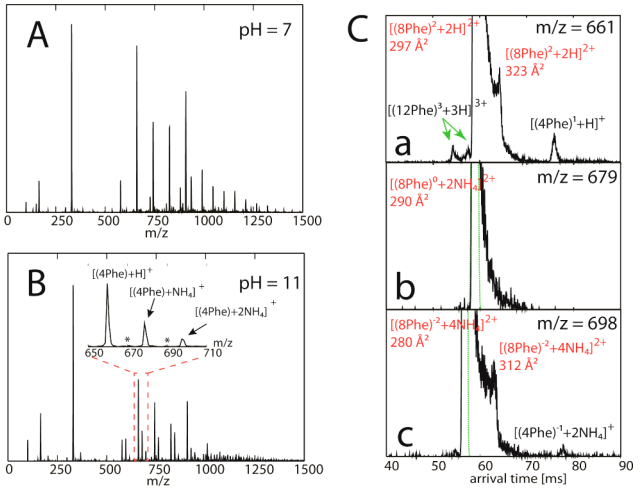

Figure 5. (A, B) ESI-q-mass spectra of 6 mM Phe in ammonium acetate buffer at pH = 7 and pH = 11. The asterisks annotate minor mass spectral peaks at 670 m/z and 688 m/z (see text for discussion). (C) Representative ATDs of the mass spectral peaks at 661, 679, and 698 m/z.

mass spectra of 6 mM Phe at pH = 7 and 11. While the mass spectrum obtained at neutral pH in ammonium acetate buffer (Figure 5A) is very similar to the spectrum obtained in water (Figure 2), the mass spectrum at pH = 11 (Figure 5B) shows the presence of ammonium cations bound to the metaclusters. For example, in addition to the parent peak at 661 m/z corresponding to $[4(\text{Phe}) + \text{H}]^+$, there are two mass spectral peaks at 679 and 698 m/z corresponding to one and two ammonium cations attached to the Phe cluster. The ATD of the parent peak at 661 m/z shows the presence of multiple features including a tetramer, two dominant octamers, and two dodecamers. The ATDs of the adduct peaks at 679 and 698 m/z are shown in panels b, c of Figure 5C. The presence of $[(8\text{Phe})^0 + 2\text{NH}_4]^{2+}$ and $[(8\text{Phe})^{-2} + 4\text{NH}_4]^{2+}$ in the ATDs of the 679 m/z and 698 m/z, and the presence of minor adduct peaks with an odd number of NH_4^+ attached (i.e., $[(8\text{Phe})^1 + \text{NH}_4]^{2+}$ and $[(8\text{Phe})^{-1} + 3\text{NH}_4]^{2+}$ at 670 m/z and 688 m/z in the mass spectrum annotated by the asterisks; see the inset of Figure 5B) indicate the protonation of the Phe-octamer is reduced from +2 (bare cluster) to +1, 0, −1, and −2 as one, two, three, and four NH_4^+ cations are added, respectively.

The stable forms of the tetramer complex are bare tetramer $[(4\text{Phe})^1 + \text{H}]^+$ and $[(4\text{Phe})^{-1} + 2\text{NH}_4]^+$ (panels a and c of Figure 5C) implying that *at least* one of the four monomers is NH_2–Phe–COO^- and that the positive charge on NH_4^+ is better coordinated by the negatively charged carboxylate COO^-.

Another interesting observation comes from the experimental cross sections of these species shown in Figure 5C. There are two octamer isomers at high pH. The dominant isomer at pH = 11 has a very similar cross section to the one recorded in water (σ = 297 vs 300 Å^2), whereas the minor isomer is significantly larger (σ = 323 Å^2). The presence of this minor isomer suggests that interactions between the neutral amino NH_2 and carboxylate COO^- terminal ends of each monomer yield more extended structures that resemble the theoretical

DOI: 10.1021/jacs.5b05482
J. Am. Chem. Soc. 2015, 137, 10080–10083

ladder-like structures obtained by Caflisch and co-workers.[7] The absence of the shoulder feature in panel b suggests that the ammonium bound ladder-like Phe octamer is not stable when the oligomer net charge is neutral. However, the experimental cross sections gradually decrease when NH_4^+ molecules adduct to the parent ion (i.e., from 323 to 312 Å^2). This result is contrary to the predictions of the simulations that indicate counterions positively contribute to the stability of ladder-like structures,[7] giving rise to a more ordered structure having a larger cross section. However, our data indicate that NH_4^+ disrupts the stability of ladder-like structures and drives the self-assembly through the same pathway that occurs at neutral pH.

A decrease in cross section of the tubular octamer with the addition of NH_4^+ (from 297 Å^2 to 290 Å^2 to 280 Å^2) indicates a structural rearrangement into a more organized, compact structure. This trend correlates well with the decrease in cross section of the same oligomer going from single, to double, and then to the tetra-tube model. Therefore, our data are consistent with a model where the presence of excess cations can induce the oligomers to grow in multiple tubes at smaller sizes than they would at neutral pH.

We note that the decrease in cross section with NH_4^+ adduction is also observed for larger metaclusters (data not shown). Therefore, two conclusions can be drawn from our data: (1) The formation of extended, ladder-like structures at high pH is driven by nonzwitterionic NH_2 and COO^- terminal interactions; these structures are relatively unstable, and (2) the presence of additional counterions may contribute negatively to the stability of those extended structures and rearrange them into more compact, pore-like structures, directing the aggregation to follow the same pathway as in the case of neutral pH. The overall results suggest that the aggregation pathway of Phe involves the formation of pore-like tetrameric oligomers. These tetramer layers stack on top of each other to elongate the structure and to take advantage of π-stacking interactions and to build multiple core structures through lateral π-stacking interactions. The toxicity of these aggregates could well arise from their hydrophobic outside surface, thus facilitating insertion into the cell membrane, coupled to their hydrophilic interior surfaces. When penetrating the cell membrane, the hydrophilic core, made of zwitterionic termini, may cause ion leakage and subsequently damage the cell.

■ ASSOCIATED CONTENT

Supporting Information

The Supporting Information is available free of charge on the ACS Publications website at DOI: 10.1021/jacs.5b05482.

Full description of materials and methods, and tables of cross sections (PDF)

■ AUTHOR INFORMATION

Corresponding Author

*bowers@chem.ucsb.edu

Present Address

[†]Department of Chemistry and Biochemistry, University of Arizona, 1306 East University Boulevard, Tucson, AZ 85721, United States.

Notes

The authors declare no competing financial interest.

■ ACKNOWLEDGMENTS

The author thanks Prof. Amedeo Caflisch at University of Zurich and Prof. Ulrich Hansmann and Helen German at University of Oklahoma for sharing their simulation results. We gratefully acknowledge support from the National Science Foundation Grant CHE-1301032 and the Air Force Office of Scientific Research Grant FA9550-11-0113 for instrumental support.

■ REFERENCES

(1) Hanley, W. B. *Am. J. Med.* **2004**, *117*, 590.
(2) Surtees, R.; Blau, N. *Eur. J. Pediatr.* **2000**, *159*, S109.
(3) Lindseth, G. N.; Coolahan, S. E.; Petros, T. V.; Lindseth, P. D. *Res. Nurs. Health* **2014**, *37*, 185.
(4) Beck, B.; Burlet, A.; Max, J. P.; Stricker-Krongrad, A. *Physiol. Behav.* **2002**, *75*, 41.
(5) Adler-Abramovich, L.; Reches, M.; Sedman, V. L.; Allen, S.; Tendler, S. J. B.; Gazit, E. *Langmuir* **2006**, *22*, 1313.
(6) Singh, V.; Rai, R. K.; Arora, A.; Sinha, N.; Thakur, A. K. *Sci. Rep.* **2014**, *4*, 3875.
(7) Adler-Abramovich, L.; Vaks, L.; Carny, O.; Trudler, D.; Magno, A.; Caflisch, A.; Frenkel, D.; Gazit, E. *Nat. Chem. Biol.* **2012**, *8*, 701.
(8) Ryan, D. M.; Anderson, S. B.; Senguen, F. T.; Youngman, R. E.; Nilsson, B. L. *Soft Matter* **2010**, *6*, 475.
(9) Griffith, E. C.; Perkins, R. J.; Telesford, D.-M.; Adams, E. M.; Cwiklik, L.; Allen, H. C.; Roeselova, M.; Vaida, V. *J. Phys. Chem. B* **2014**, in press, 10.1021/jp508473w.
(10) German, H. W.; Uyaver, S.; Hansmann, A. U. *J. Phys. Chem. A* **2015**, *119*, 1609.
(11) Bernstein, S. L.; Dupuis, N. F.; Lazo, N. D.; Wyttenbach, T.; Condron, M. M.; Bitan, G.; Teplow, D. B.; Shea, J.-E.; Ruotolo, B. T.; Robinson, C. V.; Bowers, M. T. *Nat. Chem.* **2009**, *1*, 326.
(12) Shi, L. Q.; Holliday, A. E.; Shi, H. L.; Zhu, F. F.; Ewing, M. A.; Russell, D. H.; Clemmer, D. E. *J. Am. Chem. Soc.* **2014**, *136*, 12702.
(13) Bleiholder, C.; Do, T. D.; Wu, C.; Economou, N. J.; Bernstein, S. S.; Buratto, S. K.; Shea, J.-E.; Bowers, M. T. *J. Am. Chem. Soc.* **2013**, *135*, 16926.
(14) Chen, S. H.; Chen, L. X.; Russell, D. H. *J. Am. Chem. Soc.* **2014**, *136*, 9499.
(15) Do, T. D.; Bowers, M. T. *Anal. Chem.* **2015**, *87*, 4245.
(16) Silveira, J. A.; Fort, K. L.; Kim, D.; Servage, K. A.; Pierson, N. A.; Clemmer, D. E.; Russell, D. H. *J. Am. Chem. Soc.* **2013**, *135*, 19147.
(17) Bleiholder, C.; Dupuis, N. F.; Wyttenbach, T.; Bowers, M. T. *Nat. Chem.* **2011**, *3*, 172.
(18) Mason, E. A.; McDaniel, E. W. *Transport Properties of Ions in Gases*; Wiley: New York, 1988.
(19) Kemper, P. R.; Dupuis, N. F.; Bowers, M. T. *Int. J. Mass Spectrom.* **2009**, *287*, 46.
(20) Wyttenbach, T.; Bowers, M. T. *J. Phys. Chem. B* **2011**, *115*, 12266.
(21) Wyttenbach, T.; Pierson, N. A.; Clemmer, D. E.; Bowers, M. T. *Annu. Rev. Phys. Chem.* **2014**, *65*, 175.
(22) Morriss-Andrews, A.; Shea, J. E. *Annu. Rev. Phys. Chem.* **2015**, *66*, 643.
(23) Bernstein, S. L.; Wyttenbach, T.; Baumketner, A.; Shea, J.-E.; Bitan, G.; Teplow, D. B.; Bowers, M. T. *J. Am. Chem. Soc.* **2005**, *127*, 2075.
(24) Gorbitz, C. H. *Chem. - Eur. J.* **2001**, *7*, 5153.
(25) Reches, M.; Gazit, E. *Science* **2003**, *300*, 625.
(26) Sawaya, M. R.; Sambashivan, S.; Nelson, R.; Ivanova, M. I.; Sievers, S. A.; Apostol, M. I.; Thompson, M. J.; Balbirnie, M.; Wiltzius, J. J. W.; MacFarlane, H. T.; Madsen, A. Ø.; Riekel, C.; Eisenberg, D. *Nature* **2007**, *447*, 453.
(27) Do, T. D.; Economou, N. J.; LaPointe, N. E.; Kincannon, W. M.; Bleiholder, C.; Feinstein, S. C.; Teplow, D. B.; Buratto, S. K.; Bowers, M. T. *J. Phys. Chem. B* **2013**, *117*, 8436.

DOI: 10.1021/jacs.5b05482
J. Am. Chem. Soc. 2015, 137, 10080−10083